Quantum Chemical Studies on Corrosion Inhibition of N-(N'-Phenylbenzenesulphonamido)-3-carboxy-4-methyl-4-(4-methylphenyl)-3-butanamide Derivatives: DFT-QSAR Approach.

SEMIRE Banjo* and OYEBAMIJI Abel Kolawole

Department of Pure and Applied Chemistry, Ladoke Akintola University of Technology, PMB 4000 Ogbomoso, Nigeria.
*E-mail: bsemire@lautech.edu.ng

Abstract: Quantum chemical calculations via B3LYP/6-31G (d.p) level were carried out on butenamide derivatives: N-[N'-(4-chlorophenyl) benzenesulphonamide]-3-carboxy-4-methyl-4-(4-methylphenyl)-3-butenamide (M1), N-(N`-(phenylbenzenesulphonamido)-3-carboxy-4-methyl-4-(4-methylphenyl)-3-butenamide (M2) and N-[N`-(4-methoxyhenyl) benezesulphonamido)-3-carboxy-4-methyl-4-(methylphenyl)-3-butenamide (M3) used as corrosion inhibitors for mild steel in acidic media. The calculated molecular descriptors such as the frontier energies, energy band gap, dipole moment, chemical potential (μ), chemical hardness (η) and global nucleophilicity (ω) were discussed in relation to the observed inhibitory efficiency for the compounds. The developed qualitative structural activity relationship (QSAR) model related the calculated molecular parameters to the corrosion efficiency; thus QSAR model predicted the experimental corrosion efficiencies.
[Semire, Banjo and Oyebamiji, Abel Kolawole. **Quantum Chemical Studies on Corrosion Inhibition of N-(N'-Phenylbenzenesulphonamido)-3-carboxy-4-methyl-4-(4-methylphenyl)-3-butanamide Derivatives: DFT-QSAR Approach.** *N Y Sci J* 2017;10(12):11-20]. ISSN 1554-0200 (print); ISSN 2375-723X (online). http://www.sciencepub.net/newyork. 2. doi:10.7537/marsnys101217.02.

Keywords: N-substituted butanamide derivatives, Molecular descriptors, DFT-QSAR

1.0 Introduction

Removal of rust and scale in industries are mostly achieved by acid solutions, few of these are acid pickling, acid descaling, oil well acidizing and industrial acid cleaning. Most commonly used acids in corrosion include hydrochloric acid, sulfuric acid and nitric acid. However, reactive metals such as iron and its alloys have a greater tendency to rust in all these acidic solutions. Therefore, the introduction of organic compounds containing heteroatoms (especially N and O) as an inhibitor efficiently safeguards the iron and its alloys against an acid attack, and this has attracted several researchers over the years (Ajmal et al., 1994; Achouri et al., 2001; Abd El-Rehim et al., 1999; Bethencourt et al., 1998; Ahamad et al., 2009; Ergun et al., 2014; Ebadi et al., 2012; Peme et al., 2015). The corrosion inhibitor adsorption is a function of the physico-chemical properties of the studied molecules like steric factor, functional group, molecular size, electron density at the donor atoms and π-orbital character of donating electrons (Hosseini et al., 2007; El-Naggar, 2007). The inhibitory efficiency has been found to be closely related to the inhibitor adsorption capability, the molecular planarity, molecular properties, and nature of the interaction between the p-orbital of inhibitors with the d-orbital of iron (Sastry, 1998; Cruz et et al., 2005; Bentiss et al., 2009; Cruz et al., 2009). Thus, organic compounds that exhibit good corrosion inhibition are those that possess the ability to donate electrons to unoccupied d-orbital of metallic surface during adsorption and at the same time have ability to accept free electrons from the metallic surface by using their anti-bonding orbital to form feedback bonds.

Nowadays, quantum chemical calculations has become popular practice in corrosion inhibition studies due to the ability to explain physical characters (electronic structure and reactivity parameters) which could contribute to inhibition (Okafor et al., 2010). Among other computational methods, density functional theory (DFT) has become a veritable method in developing new criteria for rationalizing, predicting and understanding chemical processes (Gece, et al., 2010). In recent times, quantum chemical calculations (especially DFT methods) have been engaged to analyze the characteristics of the inhibitor/surface mechanism and to describe the structural nature of inhibitor on the corrosion process either as a complementary method to augment the experimental results or as a sole method employed (Rodríguez-Valdez, et al., 2004; Blajievet, al., 2004; Jamalizadeh, et al., 2009; Semire, et al., 2013; Yang, et al., 2005, Bentiss, et al., 2011).

Therefore, quantum chemical calculations using density functional theory (DFT) method were performed on three butanamide derivatives i.e. N-[N'-(4-chlorophenyl) benzenesulphonamide]-3-carboxy-4-methyl-4-(4-methylphenyl)-3-butenamide (M1), N-(N`-(phenylbenzenesulphonamido)-3-carboxy-4-methyl-4-(4-methylphenyl)-3-butenamide (M2) and N-[N`-(4-methoxyhenyl) benezesulphonamido)-3-carboxy-4-methyl-4-(methylphenyl)-3-butenamide

(M3) as shown in Figure 1. These compounds have been studied experimentally to be corrosion inhibition efficient with efficiencies ranging from 82 – 96% (Khalifa et al., 2011). Thus, the major aim of this paper is to use density functional theory (DFT) to calculate molecular descriptors that relate to the observed inhibition efficiencies of these butenamide derivatives as well as to develop quantitative structural activity relationship (QSAR) model from the calculated descriptors that could predict the observed inhibition efficiencies.

M1

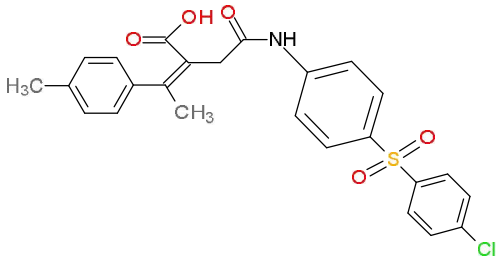

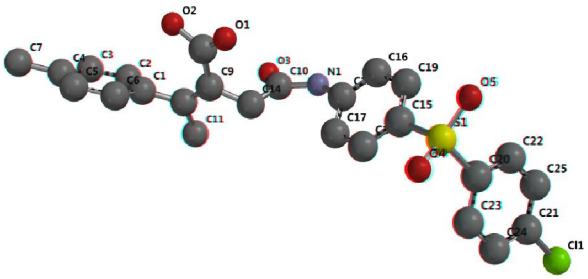

N-[N'-(4-chlorophenyl) benzenesulphonamide]-3-carboxy-4-methyl-4-(4-methylphenyl)-3-butenamide

M2

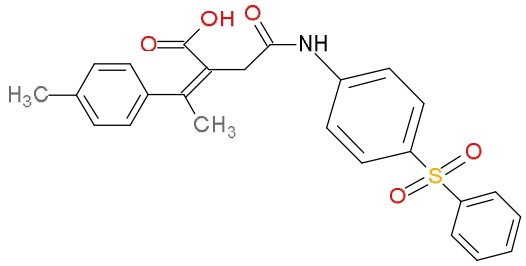

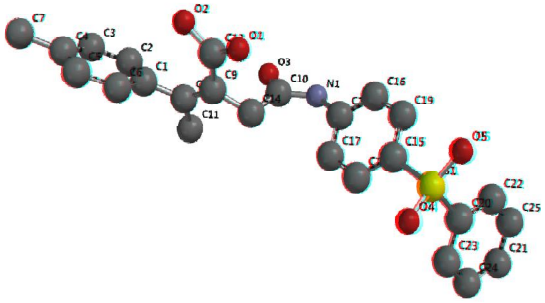

N-(N`-(phenylbenzenesulphonamido)-3-carboxy-4-methyl-4-(4-methylphenyl)-3-butenamide

M3

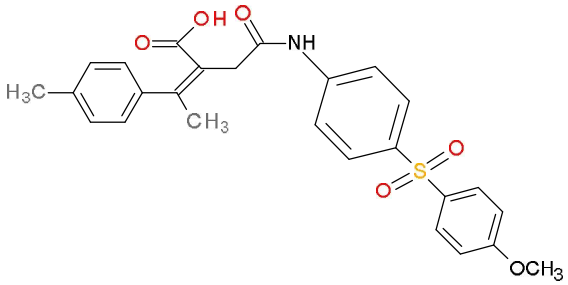

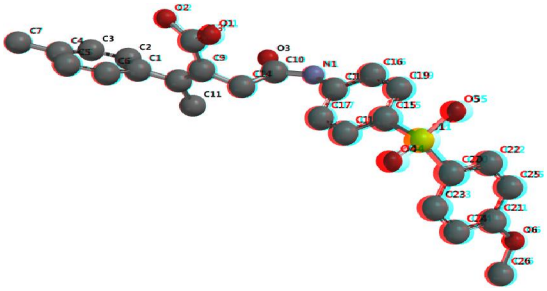

N-[N`-(4-methoxyhenyl) benezesulphonamido)-3-carboxy-4-methyl-4-(methylphenyl)-3-butenamide

Figure 1: Schematic and optimized structures with numbering of the examined compounds

2.0

Computational details

The butenamide derivatives examined in this paper were optimized using density functional theory (DFT) method with Beckes's three-parameter hybrid functional employing the Lee, Yang and Parr correlation functional B3LYP (Lee, et al., 1988; Becke, 1993). The combination of DFT and 6-31G (d,p) is known to produce good estimate of molecular properties related to molecular reactivity (Bentiss, et al., 2011). The calculated molecular parameters using DFT/6-31G (d,p) include energy of the highest molecular orbital (HOMO), energy of lowest unoccupied molecular orbital (LUMO), dipole moment, energy, chemical hardness, chemical potential and global nucleophilicity.

The chemical potential and electronegativity are related as:

$$\mu = \frac{\partial E}{\partial n} V(r) = -\chi = -\frac{IP+EA}{2} = \frac{E_{HOMO}+E_{LUMO}}{2} \quad (1)$$

where E: is the total energy, μ: chemical potential, N: number of electrons and $V(r)$: external potential of the system.

Also chemical hardness (η) is defined within the DFT as the second derivative of the energy (E) with respect to (N) as $V(r)$ property which measures both stability and reactivity of the molecule as:

$$\mu = \frac{\partial^2 E}{\partial^2 n} V(r) = -\frac{IP+EA}{2} = \frac{E_{HOMO}+E_{LUMO}}{2} \quad (2)$$

where *IP*: is the requisite quantity of energy to confiscate one electron from each atom in a mole of gaseous atom to produce one mole of gaseous ion with positive charge in the molecule, which is termed ionization potential. This is approximate to $-E_{HOMO}$; *EA*: is the energy change that occurs when a gaseous atom acquires an electron to form a univalent negative ion, which is termed electron affinity, this is approximate to $-E_{LUMO}$ (Khalifa et al., 2011; Lee et al., 1988; Becke 1993; Perez et al., 2007). The global electrophilicity is calculated by

$$\omega = \frac{\mu^2}{2\eta} \quad \textbf{(3)}$$

Electron transfer (ΔN): The number of electrons transfer is calculated using:

$$\Delta N = \frac{\chi_{Fe} - \chi_{inh}}{2(\eta_{fe} - \eta_{inh})} \quad \textbf{(4)}$$

where χ_{Fe} and χ_{inh} are absolute electronegativity of the metal (Fe) and inhibitor molecule respectivity, η_{Fe} and η_{inh} are the absolute hardness of iron and the inhibitor molecule respectively. The value of χ_{Fe} = 7.0 eV and η_{Fe} = 0 for the computation electron transferred.

Local electropilicity / nucleopilicity index: This is used to determine the reactivity of individual atom in the molecule as well as their effects in corrosion inhibition for a particular metal. It determines the change in electron density for a nucleophile $f^{+}_{(r)}$ and $f^{-}_{(r)}$ as the Funki functions which can be calculated by the finite differences approximation (Zhou et al., 1990);

$f_k^{+}{}_{(r)} = q_kN+1_{(r)} - q_kN_{(r)}$ (for nucleopilic attack) **(5)**

$f_k^{-}{}_{(r)} = q_kN_{(r)} - q_kN-1_{(r)}$ (for electrophilic attack) **(6)**

where $q_kN+1_{(r)}$, $q_kN_{(r)}$ and $q_kN-1_{(r)}$ are the electronic densities of anionic, neutral and cationic species respectively.

3.0 Results and Discussion

3.1 Quantum chemical molecular descriptors

The calculated molecular descriptors for these butenamide compounds are solvation energy, weight, hydrophobicity (Log P), volume (V), Area, polar surface area (PSA), ovality, dipole moment (DM), heteroatoms (average of Mulliken charges on all heteroatoms), HOMO (Highest occupied molecular orbital) and LUMO (Lowest unoccupied molecular orbital) as shown in Table 1. The energy of HOMO (E_{HOMO}) relates to the areas in the compound with the most active electrons; thus higher values of E_{HOMO} are likely to indicate a tendency of the molecule to donate electrons to appropriate acceptor molecules, the electrons lacking species are possibly to receive these electrons (Koopmans, 1934). Therefore, calculated energies of HOMO for the compounds are -6.32, -6.18 and -6.20 eV for **M1, M2** and **M3** respectively. The calculated HOMO energy for **M2** (-6.18 eV) should donate electrons more easily than **M1** and **M3, thus** M2 should act as a better corrosion inhibitor and it should be a preferred inhibitor in the series but **M3** presents as a better inhibitor as shown in the Table 1. This means that the trend in the E_{HOMO} values of the examined butenamide derivatives do not agree completely with the trend in the inhibition efficiencies of the compounds (Semire et al., 2013; Oguike et al., 2013; Abdulazeez et al., 2016). Likewise, the LUMO energy (E_{LUMO}) on the other hand gives information on the area in the molecule that has the uppermost propensity to receive electrons (usually the unoccupied orbital of a metal in the case) from species that are electron rich. The LUMO energies are calculated to be -1.62 eV for **M1**, -1.57 eV for **M2** and -1.47 eV for **M3**. Similarly, the trend in energy of LUMO for these compounds are not in agreement with the observed inhibition efficiency.

Table 1: Selected molecular parameters obtained by B3LYP/6-31G**

Mol	HOMO (eV)	LUMO (eV)	SE	ΔE_{H-L}	DM (Debye)	η	MW (amu)	Ovality	ΔN	%IE
M1	-6.32	-1.62	-77.56	4.70	5.13	2.35	483.97	1.68	0.845	82.20
M2	-6.18	-1.57	-72.37	4.61	4.44	2.31	444.53	1.64	0.841	86.43
M3	-6.20	-1.47	-84.34	4.73	6.26	2.37	479.55	1.69	0.811	96.30

η = Chemical hardness, MW = Molecular weight, %IE=inhibition efficiency, DM = Dipole Moment, BG = Band gap, SE = Solvation energy.

Moreover, in accordance to frontier molecular orbital theory (FMO) of chemical activity, movement of electron is a function of collaboration in-between HOMO and LUMO of retorting species, since both the energies of the HOMO and LUMO show measurable facts about the excitation properties of compounds (Semire et al., 2013; Yang et al., 2005; Abdulazeez et al., 2016; Bouachrine et al., 2009). Therefore, the strength required by the inhibitor to be fastened to the metal surface should thrive with increasing in HOMO and decreasing in LUMO energies, since an inhibitor with greater HOMO energy can simply provide electrons for metallic substrate to adsorb on its surface (Udhayakala et al., 2012; Soltani et al., 2012; El

Adnani et al., 2013; Morad et al., 2006). The energy band gap (ΔE = ELUMO – EHOMO),) gives information about the reactivity of a compound and as expected, M2 with lowest value of ΔE (4.61 eV) should be the compound with highest inhibition efficiency; since the smaller the ΔE value, the greater the reactivity of a compound (Eddy et al., 2010). On the contrary, the overall trend in the ΔE values of these compounds show no correlation with the trend in the observed inhibition efficiencies.

Furthermore, the magnitude of dipole moment is related to some extent to the polarity of the molecule and it is also a good reactivity indicator. However, it has been argued that there is no distinct relationship between dipole moment and inhibition efficiency. For instance, it has been stated that dipole moment increases with the increasing in inhibition efficiency of the inhibitors (Eddy et al., 2011). Although in another work of the same authors, he suggested that dipole moment should decrease with the increase in the inhibition efficiency of the inhibitors (Eddy et al., 2011). To make clear this inconsistency, Obi-Egbedi *et al.,* (2011) have suggested that there is no valid correlation between dipole moment and corrosion inhibition efficiency of the inhibitors (Obi-Egbedi et al., 2011). In this present study the calculated dipole moments do not show univocal trends with the inhibition efficiencies of the inhibitors (Table 1).

More so, dipole moment which is a good reactivity pointer reveals information on the molecule polarization and as reported by Eddy *et al.,* (2011) that the high inhibition efficiency of a molecule can be accredited to dipole moment with a high value and low value of band gap (Eddy et al., 2011). The resulted high dipole moment together with the low band gap shows the transfer of electron from **M** molecules to the surface which occur during adsorption to the carbon steel surface (Hong et al.,2012). Therefore, **M3** (band gap (4.73eV) and dipole moment (6.26 Debye)) agreed well with it and this made **M3** to have higher inhibition efficiency.

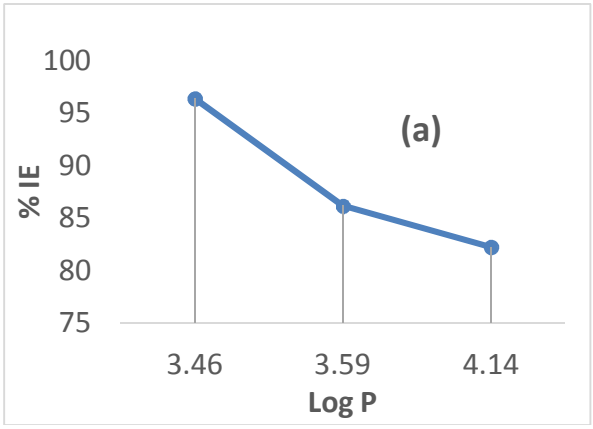

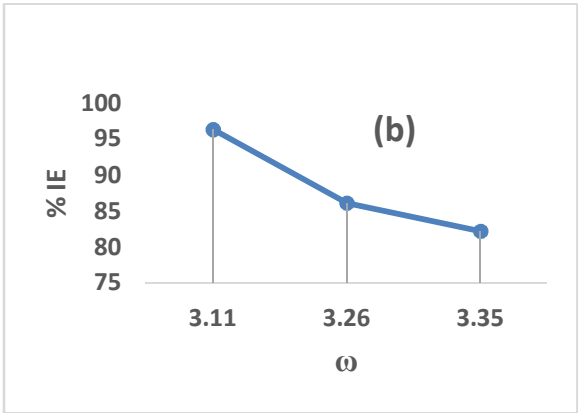

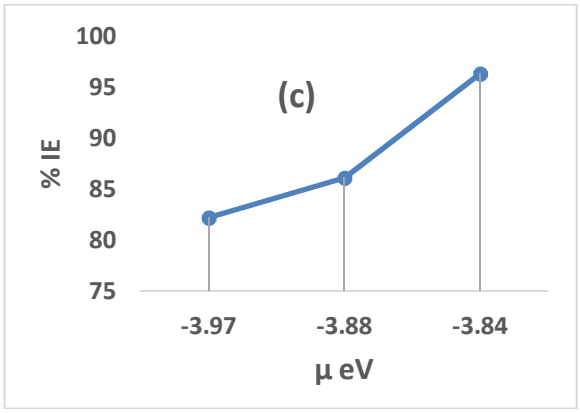

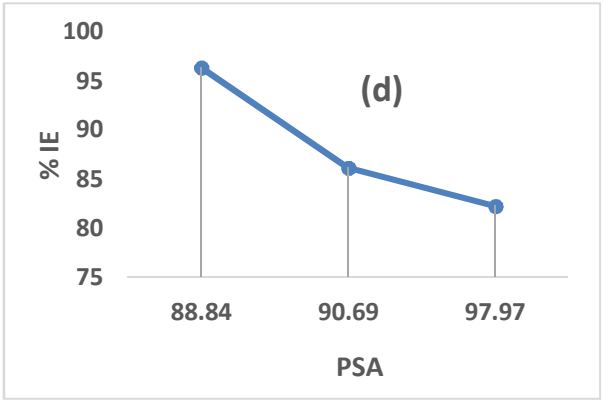

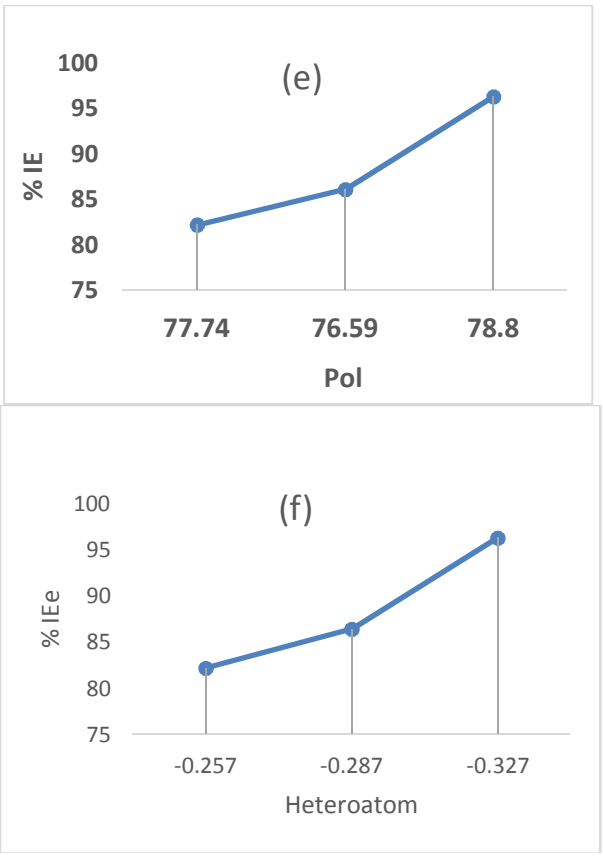

Figure 2: Relationship between some descriptors and corrosion inhibition efficiency (%IE): (a) Log P, (b) Global Nucleophilicity (ω), (c) Chemical Potential (μ), (d) Polar surface Area (PSA) and (e), Polarizability (Pol)

The ΔN is attributed to theoretical fraction of electrons that a molecule can donate electrons to the accepting molecule; thus the higher the value of ΔN, the greater the tendency of a molecule to donate electrons to the electron poor species. Thereto, in corrosion inhibiting chemistry, a higher ΔN implies a greater tendency to interact with the metal surface (i.e., a greater tendency to adsorb on the metal surface) indicating increase in inhibition efficiency (Obi-Egbedi etal., 2011; Lukovits et al., 2001). Although, in this paper, the trend in the ΔN values correlated inversely with the trend in the experimentally determined inhibition efficiency (Abdulazeez et al., 2016). Likewise, there is no relationship in the area, ovality, volume, weight with observed corrosion inhibition efficiency but other descriptors like chemical potential (μ), global nucleophilicity (ω), polarizability (Pol) and polar surface area (PSA) do have clear relationship. The ω, Log P and PSA established an inverse relationship with the observed %IE (i.e. increasing with decreasing % IE), whereas Pol, μ and heteroatom (average electronic charges on all heteroatoms) increasing with increasing in %IE as shown is Figure 2.

Mulliken population analysis is frequently used for the calculation of the charge distribution density over the molecule, this has been a suitable parameter to guesstimate the adsorption centres of inhibitors. The charge density on O1, O2, O3, O4, O5 and N for M1 are:

-0.481, -0.485, -0.487, -0.555, -0.555, -0.621*e* respectively. For M2, the charge density on O1, O2, O3, O4, O5 and N are -0.471, -0.483, -0.495, -0.569, -0.523 and -0.612*e* respectively. Also for M3, the charge density on O1, O2, O3, O4, O5, O6 and N are -0.477, -0.483, -0.472, -0.569, -0.557, -0.534 and -0.664*e* respectively (Tables 2, 3 and 4). It is usually agreed that the more negatively charged a heteroatom, the more probability its can be adsorbed on the metallic surface (Breket et al., 2002); therefore zones containing N and O are most probable sizes for adsorption of the inhibitor on the metallic surface.

The local selectivity of an inhibitor in relation to the local active sites (i.e. electrophilic and nucleophilic sites of attacks) on the molecule at which a particular reaction is likely to occur is analysed using Fukui functions. These functions give information about which atom in a molecule have a higher tendency to either donate or accept an electron. The Fukui functions for each atom in the butenamide compounds examined are listed in Tables 2, 3 and 4 for M1, M2 and M3 respectively. The f^- measures reactivity of an atom with respect to electrophilic attack (i.e. the characteristic of the molecule to donate electrons) and f^+ measures reactivity related to nucleophilic attack (i.e. the propensity of the molecule to accept electrons). The local reactivity calculated for inhibitor M1 by means of condensed Fukui functions reveal that the most probable site for nucleophilic and electrophilic attack are on chlorine atom (Cl) and C13 with 0.082 and 0.926*e* respectively (Table 2). For M2, the Fukui functions calculated show that nucleophilic and electrophilic centres are on C18 and C13 with 0.578 and 0.206*e* respectively, whereas for M3 (Table 3), it is calculated to be on C21 and C25 with 0.400 and 0.659*e* for nucleophilic and electrophilic centres respectively.

Table 2: Fukui indices for nucleophilic and electrophilic sites on inhibitor M1 calculated using Natural and Mulliken electronic charges.

Atom	q_kN	q_kN+1	q_kN-1	f_k^-	f_k^+

Atom	q_kN	q_kN+1	q_kN-1	f_k^-	f_k^+
C (1)	0.590	-0.115	0.592	0.002	-0.705
C (2)	0.019	-0.099	0.012	-0.007	-0.118
C (3)	0.544	-0.084	0.509	-0.035	-0.628
C (4)	0.066	-0.096	0.124	0.058	-0.162
C (5)	-0.362	-0.188	-0.366	-0.004	0.174
C (6)	-0.366	-0.077	-0.366	0.000	0.289
C (7)	0.075	-0.185	0.049	-0.026	-0.260
C (8)	0.128	-0.084	0.134	0.006	-0.212
C (9)	-0.108	-0.140	-0.068	0.040	-0.032
C (10)	-0.093	-0.118	-0.095	-0.002	-0.025
C (11)	-0.126	-0.103	-0.098	0.028	0.023
C (12)	-0.124	0.307	-0.108	0.016	0.431
C (13)	-0.382	0.544	-0.388	-0.006	**0.926**
C (14)	0.319	0.341	0.349	0.030	0.022
C (15)	-0.174	0.114	-0.157	0.017	0.288
C (16)	-0.088	0.490	-0.081	0.007	0.578
C (17)	-0.110	-0.354	-0.117	-0.007	-0.244
C (18)	-0.08	-0.016	-0.068	0.012	0.064
C (19)	-0.095	-0.124	-0.093	0.002	-0.029
C (20)	-0.172	-0.086	-0.173	-0.001	0.086
C (21)	-0.089	-0.119	-0.085	0.004	-0.030
C (22)	-0.077	-0.376	-0.074	0.003	-0.299
C (23)	-0.072	-0.125	-0.064	0.008	-0.053
C (24)	-0.067	-0.084	-0.067	0.017	-0.017
C (25)	-0.067	-0.079	-0.065	0.002	-0.012
C (26)	0.066	-0.188	-0.667	0.000	-0.254
O (1)	-0.481	-0.575	-0.452	0.061	-0.094
O (2)	-0.495	-0.574	-0.466	0.029	-0.079
O (3)	-0.487	-0.504	0.487	-0.974	-0.017
O (4)	-0.555	-0.542	-0.518	-1.073	0.013
O (5)	-0.555	-0.462	-0.519	0.036	0.093
Cl	-0.002	-0.077	0.08	**0.082**	-0.075
N	-0.621	-0.672	-0.599	0.022	-0.051
S	1.142	1.069	1.134	-0.008	-0.073

Table 3: Fukui indices for nucleophilic and electrophilic sites on inhibitor M2 calculated using Natural and Mulliken electronic charges.

Atom	q_kN	q_kN+1	q_kN-1	f_k^+	f_k^-
C (1)	0.016	-0.109	0.008	-0.125	0.008
C (2)	0.511	-0.091	0.496	-0.602	0.015
C (3)	0.054	-0.082	0.100	-0.136	-0.046
C (4)	-0.300	-0.085	-0.307	0.215	0.007
C (5)	-0.500	-0.106	-0.555	-0.606	0.055
C (6)	-0.360	-0.181	-0.367	0.179	0.007
C (7)	0.168	-0.138	0.030	-0.306	0.138
C (8)	-0.036	-0.087	0.133	-0.051	-0.169
C (9)	-0.118	0.294	-0.077	0.412	-0.041
C (10)	-0.109	-0.193	-0.084	-0.084	-0.025
C (11)	-0.126	0.501	-0.099	0.627	-0.027
C (12)	-0.127	-0.130	-0.140	-0.003	0.013
C (13)	-0.182	-0.283	-0.388	-0.101	**0.206**
C (14)	0.279	0.105	0.344	-0.174	-0.065
C (15)	-0.175	0.492	-0.155	0.667	-0.020
C (16)	-0.077	-0.352	-0.089	-0.275	0.012
C (17)	-0.085	0.105	-0.112	0.190	0.027
C (18)	-0.086	0.492	-0.069	**0.578**	-0.017
C (19)	-0.090	0.005	-0.035	0.095	-0.055
C (20)	-0.171	0.013	-0.174	0.184	0.003
C (21)	-0.075	-0.098	-0.065	-0.023	-0.010
C (22)	-0.081	-0.095	-0.065	-0.014	-0.016
C (23)	-0.076	-0.127	-0.082	-0.051	0.006
C (24)	-0.085	-0.124	-0.078	-0.039	-0.007
C (25)	-0.085	0.121	-0.080	0.206	-0.005
C (26)	-0.305	-0.377	-0.250	-0.072	-0.055

O (1)	-0.471	-0.577	-0.427	-0.106	-0.044
O (2)	-0.483	-0.562	-0.436	-0.079	-0.047
O (3)	-0.495	-0.586	-0.467	-0.091	-0.028
O (4)	-0.569	-0.451	-0.521	0.118	-0.048
O (5)	-0.523	-0.487	-0.511	0.036	-0.012
N	-0.612	-0.590	-0.577	0.022	-0.035
S	1.146	1.056	1.123	-0.090	0.023

Table 4: Fukui indices for nucleophilic and electrophilic sites on inhibitor M3 calculated using Natural and Mulliken electronic charges.

Atom	**q_kN**	**q_kN+1**	**q_kN-1**	**f_k^+**	**f_k^-**
C (1)	0.016	-0.007	0.010	-0.023	0.006
C (2)	0.511	0.508	0.165	-0.003	0.346
C (3)	0.054	-0.275	-0.292	-0.329	0.346
C (4)	-0.300	0.083	0.081	0.383	-0.381
C (5)	0.560	0.507	0.510	-0.053	0.050
C (6)	-0.360	-0.352	-0.366	0.008	0.006
C (7)	0.065	0.026	0.032	-0.039	0.033
C (8)	0.128	0.004	0.132	-0.124	-0.004
C (9)	-0.118	-0.113	-0.112	0.005	-0.006
C (10)	-0.109	-0.089	-0.081	0.020	-0.028
C (11)	-0.126	-0.124	-0.106	0.002	-0.020
C (12)	-0.382	-0.124	-0.107	0.258	-0.275
C (13)	-0.382	-0.275	-0.387	0.107	0.005
C (14)	0.279	0.281	0.337	0.002	-0.058
C (15)	-0.175	-0.195	-0.161	-0.020	-0.014
C (16)	-0.077	-0.116	-0.081	-0.039	0.004
C (17)	-0.085	-0.142	-0.119	-0.057	0.034
C (18)	-0.086	-0.090	-0.070	-0.004	-0.016
C (19)	-0.090	-0.123	-0.096	-0.033	0.006
C (20)	-0.171	-0.181	-0.169	-0.010	-0.002
C (21)	-0.075	0.325	0.376	**0.400**	-0.451
C (22)	-0.081	-0.101	-0.082	-0.020	0.001
C (23)	-0.076	-0.088	-0.074	-0.012	-0.002
C (24)	-0.085	-0.139	-0.116	-0.054	0.031
C (25)	0.560	-0.122	-0.099	-0.682	**0.659**
C (26)	-0.086	-0.066	-0.110	0.020	0.024
O (1)	-0.477	-0.573	-0.451	-0.096	-0.026
O (2)	-0.483	-0.457	-0.469	0.026	-0.014
O (3)	-0.472	-0.455	-0.482	0.017	0.010
O (4)	-0.569	-0.580	-0.521	-0.011	-0.048
O (5)	-0.557	0.575	-0.514	1.132	-0.043
O (6)	-0.534	-0.578	-0.521	-0.044	-0.013
N	-0.664	-0.612	-0.602	0.052	-0.062
S	1.137	1.056	1.126	-0.081	0.011

3.2 *QSAR model using Multiple Linear Regressions*

Quantitative structural activity relationship (QSAR) as a geometric model relates a set of structural descriptors of a chemical compound to its biological activity (Hansch, 1969). QSAR is developed to relate the molecular descriptors from quantum chemical calculations of the examined butanmide derivatives to the observed %IE of the corrosion inhibitors. In this technique of analysis, the model quality depends on the fitting and prediction ability. Therefore, it is appropriate to establish a relationship in the form of a linear equation that connects the indices of the quantum chemical molecular parameters/desscriptors to the experimentally determined inhibition efficiencies. The linear equation postulated by Lukovits (2001) is frequently used to correlate the quantum molecular descriptors of corrosion inhibitors with the % experimental inhibition efficiency (Lukovits et al., 2001). In order to build QSAR model and test the model workability, the data are divided into set which

in building the model. The linear model is built using selected descriptors from the data set to obtain the following linear equation represented in Equation 7.

$$\%IE = \acute{\alpha} + \beta_1 X_1 + \beta_2 X_2 ..... \beta_n X_n \quad \textbf{(7)}$$

Where ά and β are constants i.e regression coefficients determined through regression analysis, X_1, X_2.... X_n are characteristic quantum chemical indices of the molecule 1, 2...n.

In addition, the validation of QSAR model can be achieved by using arithmetic equations in order to consider cross validation (R^2). Cross validation controls how dependable a QSAR model can be employed for a set of data. It is also used as a logical device to assess the extrapolative power of an equation. Therefore, Equation (8) could be used.

$$CV.\boldsymbol{R^2} = \mathbf{1} - \frac{\Sigma(Yobs - Ycal)^2}{\Sigma(Yobs - \bar{Y}obs)^2} \quad \textbf{(8)}$$

The correlation between the corrosion efficiency and all the molecular descriptors are discussed and the corrosion efficiency is positively correlated to some of the descriptors. For example; corrosion efficiency is positively correlated to chemical hardness (η) by 0.545 as well as polarizability by 0.67; meanwhile it is negatively correlated to global nucleophilicity by -1.000 as well as log P by -0.834. Similarly, some of the descriptors are also correlated to one another, e.g., polarizability is positively correlated to chemical hardness by 0.986 and log P is positively correlated to global nucleophilicity by 0.826 while global nucleophilicity is negatively correlated to chemical hardness by -0.556 and polarizability is negatively correlated to global nucleophilicity by -0.687 as shown in Table 5. Therefore, the choice of effective molecular descriptors for valid analysis is a function of Pearson correlation, though the making of reliable model involved huge quantity of molecules. Moreover, the inhibitory activity of three experimental molecules is prodded into and two molecular descriptors are selected among the calculated molecular descriptors in order to avoid multi-collinearity as shown in Equation 9. Also, Figure 3 shows the effectiveness of the established QSAR model as experimental %IE are well reproduced.

Table 5: Pearson's correlation matrix for descriptors

	%IE	**η**	**ω**	**Log P**	**Pol**
%IE	1.000				
η	0.545	1.000			
ω	-1.000	-0.556	1.000		
Log P	-0.834	0.009	0.826	1.000	
Pol	0.676	0.986	-0.687	-0.157	1.000

Stepwise regression result for anticorrosion activity	R^2	CV. R^2
%IE = -139.932 - 14.901 (Log P) + 3.648 (Pol) **---------9**	.09998	0.999

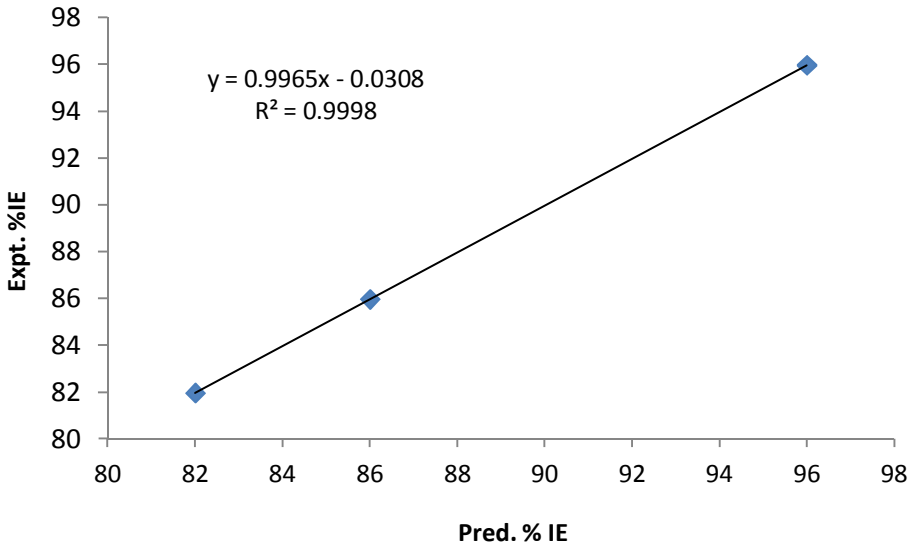

Figure 3: Correlation between experimental and predicted % IE

The %IE predicted through QSAR model are replicative of the experimental %IE as shown in Figure 3 with fitting factor (R^2) is 0.9998. This shows that the QSAR model replicates the observed % IE of these compounds. Therefore, the combination certain descriptors such as of log P and polarizability described the inhibitory activity of the studied compounds.

Moreover, as shown in Table 5, regression parameters (R^2, CV.R^2) were calculated for the studied

molecules in order to validate the QSAR model developed for inhibitory activity. The R^2 which is equal to 0.9998 showed a promising fitness and this revealed the efficiency of the developed model (Equation 9). Also, the value for calculated $CV.R^2$ was observed to be closer to 1.00 (> 0.5 (standard)) (Marrero et al., 2004) which indicates its reliability and acceptability, therefore, the developed QSAR model have a promising prognostic power.

Conclusion

Density Functional theory via B3LYP/6-31G** method has been used to calculate molecular descriptors/parameters such as E_{HOMO}, E_{LUMO}, $\Delta E_{HOMO-LUMO}$ (energy gap), chemical hardness (η), chemical potential (μ), the fraction of electron transferred (ΔN) and (ω) for the butenamide 'derivatives. The calculations revealed that electrophilicity index (ω), Log P and polar surface area (PSA) decreased in values with increasing in the observed %IE; whereas polarizability (pol). Heteroatoms (average electronic charges on all heteroatoms) and chemical potential (μ) increased with increasing in %IE. The selected molecular descriptors calculated are used to develop QSAR model that fitted into experimentally determined corrosion efficiency. The QSAR model reproduced the experimental %CI.

Reference

1. Abd El-Rehim S.S., Ibrahim M.A.M., Khalid K.F. 4-Aminoantipyrine as an inhibitor of mild steel corrosion in HCl solution. J Appl Electrochem 1999; 29:593– 599.
2. Abdulazeez M.O., Oyebamiji A.K. and Semire B. DFT-QSAR studies on corrosion inhibition efficiency of derivatives of thiadiazole, oxadiazole and triazole. International Journal of Corrosion and Scale Inhibition 2016;5(3): 248–262. doi: 10.17675/2305-6894-2016-5-3-5.
3. Ahamad I., Quraishi M.A., Bis (benzimidazol-2-yl) disulphide: An efficient water soluble inhibitor for corrosion of mild steel in hydrochloric acid media. Corros Sci 2009; 51: 2006–2013.
4. Ajmal M., Mideen A.S., Quraishi M.A., 2-Hydrazino-6-methyl-benzothiazole as an effective inhibitor for the corrosion of mild-steel in acidic solutions. Corros Sci 1994; 36: 79–84.
5. Becke A. Density functional thermochemistry. III. The role of exact exchange. Journal of Physical Chemistry 1993; 98: 5648 – 5652.
6. Bentiss F. and Lagrenée M. Heterocyclic compounds as corrosion inhibitors for mild steel in hydrochloric acid medium — correlation between electronic structure and inhibition efficiency. Journal of Material Environmental Science 2011; 2(1): 13-17.
7. Bentiss F., Jama C., Mernari B., El Attari H., El Kadi L., Lebrini M., Traisnel M and Lagrenee M. Corrosion control of mild steel using 3,5-bis (4-methoxyphenyl)-4-amino-1,2,4-triazole in normal hydrochloric acid medium. Corros Sci 2009; 51:1628-1635.
8. Bethencourt M., Botana F.J., Calvino J.J., Marcos M., Rodriguez-chacon M.A. Lanthanide compounds as environmentally friendly corrosion inhibitors of aluminum alloys: A review. Corros. Sci 1998;40: 1803– 1819.
9. Blajiev O and Hubin A. Inhibition of copper corrosion in chloride solutions by amino-mercapto-thiadiazole and methyl-mercapto-thiadiazole: an impedance spectroscopy and a quantum chemical investigation. Electrochim Acta 2004;49: 2761–2770.
10. Bouachrine M., Hamidi M., Bouzzine S.M., and Taoufik H. Theoretical study on the structure anaelectronic properties of new materials based on thiophene and oxadiazole. Journal of Chemical Research 2009;10: 29-37.
11. Breke G., Hur E. and Ogretir C. Quantum chemical studies of some pyridine derivatives as corrosion inhibitor in acidic medium. J Mol Struct (THEOCHEM) 2002; 578:79-88.
12. Cruz J., Martinez-Aguilera L.M.R., Salcedo R and Castro M. Reactivity properties of derivatives of 2-imidazoline: an ab initio DFT study. Int J Quantum Chem 2001;85:546-556.
13. Cruz J., Pandiyan T. and Garcia-Ochoa E. A new inhibitor for mild carbon steel: Electrochemical and DFT studies. J Electroanal Chem 2005;583: 8-16.
14. Domingo L. R., Aurell M., Contreras M and Perez P. Quantitative Characterization of the Local Electrophilicity of Organic Molecules. Understanding the Regioselectivity on Diels−Alder Reactions. J Phys Chem A 2002;106:6871-6876.
15. Ebadi, M., Basirun, W.J., Khaledi, H., Ali, H.M. Corrosion inhibition properties of pyrazolylindolenine compounds on copper surface in acidic media. Chem Central J 2012; 6: 163. Doi: 10.1186/1752-153X-6-163.
16. Eddy N.O, Awe F.E, Gimb C.E, Ibisi N.O and Ebenso E.E. QSAR, experimental and computational chemistry simulation studies on the inhibition potentials of some amino acids for the corrosion of mild steel in 0.1 M HCl. Int Journal of Electrochem. Sci., 2011; 6: 931-957.
17. Eddy N.O. Adsorption and Quuantum chemical studies on cloxallin and Halides for the corrosion of mild steel in acidic medium. Int J Electrochemical Science 2010;39(5): 288-295.
18. Eddy N.O., Awe F.E, Gimba, C.E, Ibisi, N.O and Ebenso, E.E. QSAR, Experimental and computational chemistry simulation studies on inhibition potential of some amino acids for corrosion of mild steel in 0.1M HCL. Int Journal of Electrochem Science 2011; 6:931-957.

19. El Achouri M., Infante M.R., Izquierdo F., Kertit S., Gouttoya H.M., Nciri B. Synthesis of some cationic Gemini surfactants and their inhibitive effect on iron corrosion in hydrochloric acid medium. Corros Sci 2001;43: 19–35.
20. El Adnani Z., Mcharfi M., Sfaira M., Benzakour M., Benjelloun A.T. and Ebn Touhami M. DFT theoretical study of 7-R-3methylquinoxalin-2(1H)-thiones (R=H: CH_3; Cl) as corrosion inhibitors in hydrochloric acid. Corros Sci 2013; 68: 223.
21. El-Naggar M.M. Corrosion inhibition of mild steel in acidic medium by some sulfa drugs compounds. Corros Sci 2007; 49: 2226.
22. Ergun U., Emregul K.C., Azole compounds as corrosion inhibitors: part 1. J. Material Eng Perform 2014; 23: 213. Doi: 10.1007/s11665-013-0737-2.
23. Gece G. and Bilgic S. A theoretical study of some hydroxamic acids as corrosion inhibitors for carbon steel. Corros Sci 2010;52:3304-3308.
24. Hansch C. A quantitative approach to biochemical structure-activity relationships. Accounts of Chemical Research 1969; 2: 232-239.
25. Hong S., Chen W., Luo H.Q., Li N.B. Inhibition effect of 4-aminoantipyrine on the corrosion of copper in 3wt.% NaCl solution. Corros Science 2012;57: 270.
26. Hosseini MG, Ehteshamzadeh M, Shahrabi T. Protection of mild steel corrosion with Schiff bases in 0.5 M H_2SO_4 solution. Electrochim Acta 2007;52:3680.
27. Jamalizadeh E., Hosseini S.M.A and Jafari A.H. Quantum chemical studies on corrosion inhibition of some lactones on mild steel in acid media. Corros Sci 2009;51:1428–1435.
28. Khalifa O.R., Abdallah. Corrrosion inhibition of some organic compounds on low carbon steel in hydrochloric acid solution. Port. Elecrochim Acta, 2011;29: 47-56.
29. Koopmans T. Ordering of Wave Functions and Eigen values to the Individual Electrons of an Atom. Physica 1934;1:104-113.
30. Lee C., Yang W., Parr R.G. Development of the colle-salvetti correlation-energy formula into a functional of the electron density. Phys Rev B 1988; 37: 785.
31. Lukovits I., Kalman E., and Zucchi, F. Corrosion Inhibitors: Correlation between Electronic Structure and Efficiency. Corros Sci 2001;57:3-8.
32. Marrero P.Y., Castillo G.J.A., Torrens F., Romero Z.V., and Castro E.A. Atom, atom-type, and total linear indices of the “molecular pseudograph's atom adjacency matrix”: application to QSPR/QSAR studies of organic compounds. Molecules 2004;9(12):1100–1123.
33. Morad M.S. and Kamal El-Dean A.M. 2,2`-Dithiobis (3-cyano-4,6-dimethylpyridine): A new class of acid corrosion inhibitors for mild steel. Corros Sci 2006;48:3398.
34. Obi-Egbedi N.O., Obot I.B., El-Khaiary M.I., Umoren S.A and Ebenso E.E. Computational simulation and statistical analysis on the relationship between corrosion inhibition efficiency and molecular structure of some phenanthroline derivatives on mild steel surface. International Journal of Electrochemical Science 2011; 6:5649-5675.
35. Oguike R.S., Kolo A.M., Shibdawa A.M and Gyenna H.A. Density Functional Theory of Mild steel corrosion in acid midie using dyes as inhibitor: Adsorption onto Fe (110) from gas phase. Phys Chem 2013:1-9.
36. Okafor P.C, Ebenso E.E and Ekpe U.J. Azadirachata indica extracts as corrosion inhibitor for mild steel in acid medium. International journal of electrochemical science 2010;5: 978-993.
37. Parr R.G., Szentpaly L and Liu S. Electrophilicity Index. J Am Chem Soc 1999;121:1922-1924.
38. Peme T., Olasunkanmi L.O., Bahadur I., Adekunle A.S., Kabanda M.M., Ebenso E.E. Adsorption and corrosion inhibition studies of some selected dyes as corrosion inhibiors for mild steel in acidic medium: Gravimetric, Electrochemical, Quantum Chemicl studies and Synergistic effect with iodine ions. Molecules. 2015; 20: 16004-16029.
39. Perez A., Luque F.J., Orozco M. Dynamics of B-DNA on the microsecond time scale. J. Am. Chem. Soc 2007;129:14739-14745.
40. Rodríguez-Valdez L.M., Martínez-Villafane A and Glossman-Mitnik D. CHIH-DFT determination of the molecular structure, infrared and ultraviolet spectra of potentially organic corrosion inhibitors. J Mol Struct (THEOCHEM) 2004;681: 83–88.
41. Sastry V.S. Corrosion Inhibitors. Principles and Applications, John Wiley & Sons, New York. 1998.
42. Semire B and Odunola O.A. Density functional theory on the efficiencies of 2-phynylimidazole (1,2-a) pyridine and 2-(M-methophenyl) imidazole (1,2-a) pyridine as corrosion inhibition on mild steel. Bulgarian Journal of Chemical Education. 2013;22(6):893-906.
43. Soltani N., Tavakkoli N., Khayatkashani M., Jalali M.R. and Mosavizade A. Green approach to corrosion inhibition of 304 stainless steel in hydrochloric acid solution by the extract of salvia officinalis leaves. Corros Sci 2012; 62: 122.
44. Udhayakala P., Rajendiran T.V and Gunasekaran S. Scholar research library theoretical approach to the corrosion inhibition efficiency of some pyridine derivatives using DFT method. J. of Comp. methods in mol des 2012;2(1):1-15.
45. Yang L., Feng J., and Ren A. Theoretical studies on the electronic and optical properties of two thiophene–fluorene based π-conjugated copolymers. Polymer 2005;46:10970-10982.
46. Yang W., and Parr R. Hardness, softness, and the fukui function in the electronic theory of metals and catalysis. Proceedings of the National Academy of

Sciences of the United States of America 1985;82: 6723–6726.

47. Zhou Z. and Navangul H.V. Absolute hardness and aromaticity: MNDO study of benzenoid hydrocarbons. J Phys Org Chem 1990;3:784-788.

11/13/2017